CrossMark

ORIGINAL RESEARCH

Correlations of NBO energies of individual hydrogen bonds in nucleic acid base pairs with some QTAIM parameters

Halina Szatylowicz[1] · Aneta Jezierska[2] · Nina Sadlej-Sosnowska[3]

Abstract DNA and RNA base-pairs are the most important systems containing multiple hydrogen bonds. Characterizing the energy of individual intermolecular interactions in such systems is vital and still an open problem that has been tackled here within the framework of the natural bond orbital (NBO) and the quantum theory of atoms in molecules (QTAIM) theories. In the NBO language, energy of an individual H-bond depends on the interaction of the n_Y, σ^*_{XH}, and σ_{XH} orbitals directly involved in H-bonding. A partial charge transfer between donor (n_Y) and acceptor (σ^*_{XH}) orbitals provides a substantial bonding contribution to the energies of the H-bonds, and in the end, the H-bonded complexes. It is accompanied with a repulsive contribution due to the proximity of the n_Y and σ_{XH} orbitals. Energies of the individual H-bonds, resulting from addition of the both terms, were correlated with several parameters, provided by the QTAIM analysis which has also been extensively used to characterize the hydrogen bond. The calculations were performed for the G–C and A–T Watson–Crick base pairs, their substituted derivatives (by one of two substituents, NH_3^+ or OH_2^+), A–U occurring in RNA and a wobble pair G–U. The best correlations were found for the NBO energy with the electron density and the potential energy density at H-bond critical points. The correlations held for the heterogeneous samples of HBs of different types, i.e. N–H···O, N–H···N, and C–H···O, occurring simultaneously in DNA base pairs.

Introduction

Due to their importance in many fields of biological chemistry, the hydrogen bonds (HBs) in DNA base pairs have been the subject of many theoretical investigations. The relative energies of two or three hydrogen bonds were estimated in a single base-pair, as well as compared in different pairs [1], e.g. A–T versus G–C. The energy of an individual H-bond has been evaluated by several approaches: (1) in the (presumed) absence of other intermolecular interactions as a bonding energy of the H-bonded complex [2]; (2) through calculations of inter-residue compliance constants for all possible X–H···Y contacts [3]; (3) by application of an atom replacement procedure [4]; (4) using the ELM (Espinosa, Lecomte, Molins) equation [5] to estimate of the individual O···H energy, whereas N···H ones obtained from the difference in the total binding energy between the two monomers and the energies of the remaining O···H interactions [6] (5) utilizing the obtained relationship between the dissociation energy of the

Dedicated to the memory of Professor Oleg V. Shishkin (1966–2014).

✉ Halina Szatylowicz
   halina@ch.pw.edu.pl

✉ Nina Sadlej-Sosnowska
   n.sadlej@nil.gov.pl

[1] Faculty of Chemistry, Warsaw University of Technology, 3 Noakowskiego St., 00-664 Warsaw, Poland

[2] Faculty of Chemistry, University of Wrocław, 14 Joliot-Curie St., 50-383 Wrocław, Poland

[3] National Medicines Institute, 30/34 Chełmska St., 00-725 Warsaw, Poland

individual intermolecular interactions and the electron density at the H-bond critical point, obtained for symmetrical complexes with two identical N–H⋯O H-bonds [7, 8]; (6) an application of the Natural Bond Orbital (NBO) concept to intermolecular interactions [9]. All these methods were described in more detail as well as their results compared in our previous paper [9]. The energies of individual H-bonds in A–T and G–C Watson–Crick pairs and in the pairs upon substitution by one of two cationic substituents (OH_2^+ or NH_3^+) were calculated according to the NBO analysis of intermolecular interactions [9].

Recently, another attempt to estimate energy of individual HBs in multiple-bonded systems has been undertaken. To this end, a magnetically induced current strength across individual HB was used [10]. For HBs in homo- and hetero-dimers of H_2O, NH_3, H_2CO, HCl and HF, a linear relation between the diamagnetic current susceptibility and the interaction energy was found. This relationship was used (as a calibration curve) to study individual HB energies in A–T and G–C Watson–Crick pairs as well as H-bonded water chains in carbonic anhydrase.

Another approach of Nikolaienko et al. [11] combined the QTAIM method with vibrational analysis and correlated a red-shift of the proton involved in H-bond with the electron density in a bond critical point. Energies of individual intermolecular HBs in A–T [12] and G–C [13] pairs as well as their tautomeric forms were estimated.

Results of the application of the both above mentioned methods revealed that the obtained sequences of the individual HB strengths in G–C and A–T pairs

($\mathbf{a} > \mathbf{b} > \mathbf{c}$ and $\mathbf{b} > \mathbf{a}$, respectively, see Scheme 1) agreed only with the results of the NBO approach (see Table 1 in Ref. [9]).

Among different physical terms contributing to the complexes binding energy, we can distinguish the terms common to all interacting molecules situated close one to another, and the terms uniquely due to the presence of H-bonds. Within the NBO theory [14], the energy of a chemical system can be divided into two parts: one associated with the localized orbitals (E_{Lewis} or E_L) and a second originating from noncovalent contributions ($E_{nonLewis}$ or E_{nL}). The latter is calculated by the perturbation theory and presented as a transfer of electron density between pairs of orbitals. For hydrogen-bonded (HB) molecules the highest value of E_{nL} (named also $E_{n-\sigma^*}$) is due to the partial charge transfer between the first "filled" bonding orbital (donor NBO, Lewis type) and the second "empty" antibonding or Rydberg (acceptor NBO, non-Lewis type). The NBO analysis emphasizes the role of the charge-transfer interactions of the $n \rightarrow \sigma^*$ type, involving a weak intermolecular delocalization from a lone pair (n) of the donor monomer into the proximate unfilled antibonding orbital σ^* of the acceptor monomer. Besides the bonding electron delocalizations, the proximity of atoms belonging to two molecules brings about steric repulsions between them [14]. The most important are steric repulsions between filled n_Y and σ_{X-H} orbitals of the X–H⋯Y interaction. Therefore, energy of the charge transfer, $E_{n-\sigma^*}$, also called delocalization energy (attractive interaction), has to be corrected by energy of the steric

Scheme 1 H-bonded complexes of nucleic acid pairs: **a** guanine–cytosine (G–C), **b** adenine–thymine (A–T), **c** guanine–uracil (G–U) and **d** adenine–uracil (A–U)

(a) Guanine-Cytosine (G-C)

(b) Adenine-Thymine (A-T)

(c) Guanine-Uracil (G-U)

(d) Adenine-Uracil (A-U)
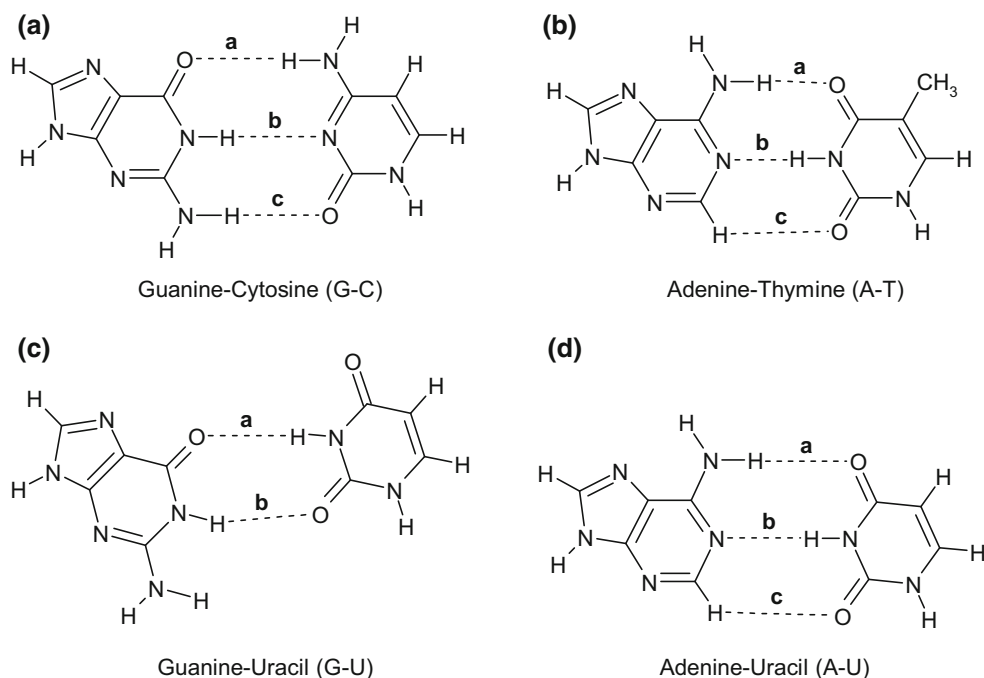
exchange repulsion [15–18] between filled n_Y and σ_{X-H} orbitals, $E_{\sigma-n}$. The sum of the attractive ($E_{n-\sigma*}$) and repulsive ($E_{\sigma-n}$) terms was used as a measure of the energy of an individual HB [9]. It characterizes well the energy increment due to the hydrogen bond by oneself in contrast to the binding energy of a complex (called also in the literature the H-bond strength, stabilization energy, or the complex interaction energy) which characterizes the complex taken as a whole. The latter, according to supramolecular approach [19], is calculated as a difference between the energy of the complex and the sum of the energies of monomers for their geometry such as in the complex. Therefore, this energy contains also contributions of interacting peripheral parts of the complex components and it ought to be emphasized that the perturbation of the electron density takes place not only in the immediate vicinity of the H and X atoms but within the entire complex [20–22]. Consequently, there are other contributions to the binding energy of the complex. In these connections, one cannot expect that the sum of the bonding and steric interactions inside the individual X–H⋯Y moieties would be equal to the bonding energy of a given pair nor it is entitled to attribute the difference to some presumed cooperative effects [2, 4].

For a pair of molecules connected by H-bond (or several H-bonds) one can also calculate a total charge transfer

Scheme 2 H-bonded complexes of substituted nucleic acid pairs: **a** guanine–cytosine (R1G-CR2), **b** adenine–thymine (R1A-TR2); R1 = NH$_3^+$ or H and R2 = H or OH$_2^+$, respectively
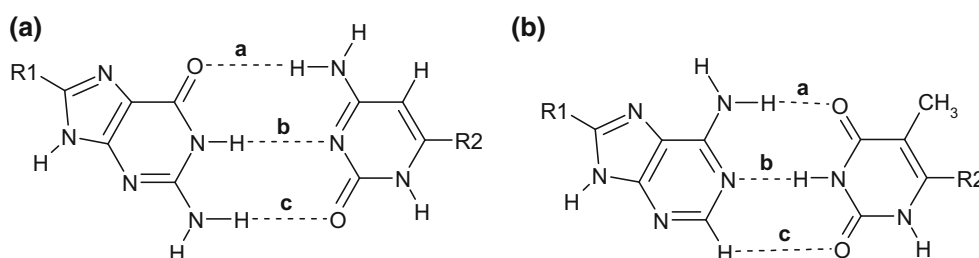

Fig. 1 Relationship between the energy of a single H-bond, E_{NBO}, and the electron density at BCP, ρ(BCP), for G–C, A–T, G–U, A–U and substituted derivatives R1G-CR2 and R1A-TR2 pairs obtained at **a** B3P86, **b** B3LYP, **c** M05-2X and **d** HF levels with 6-311++G(d,p) basis set
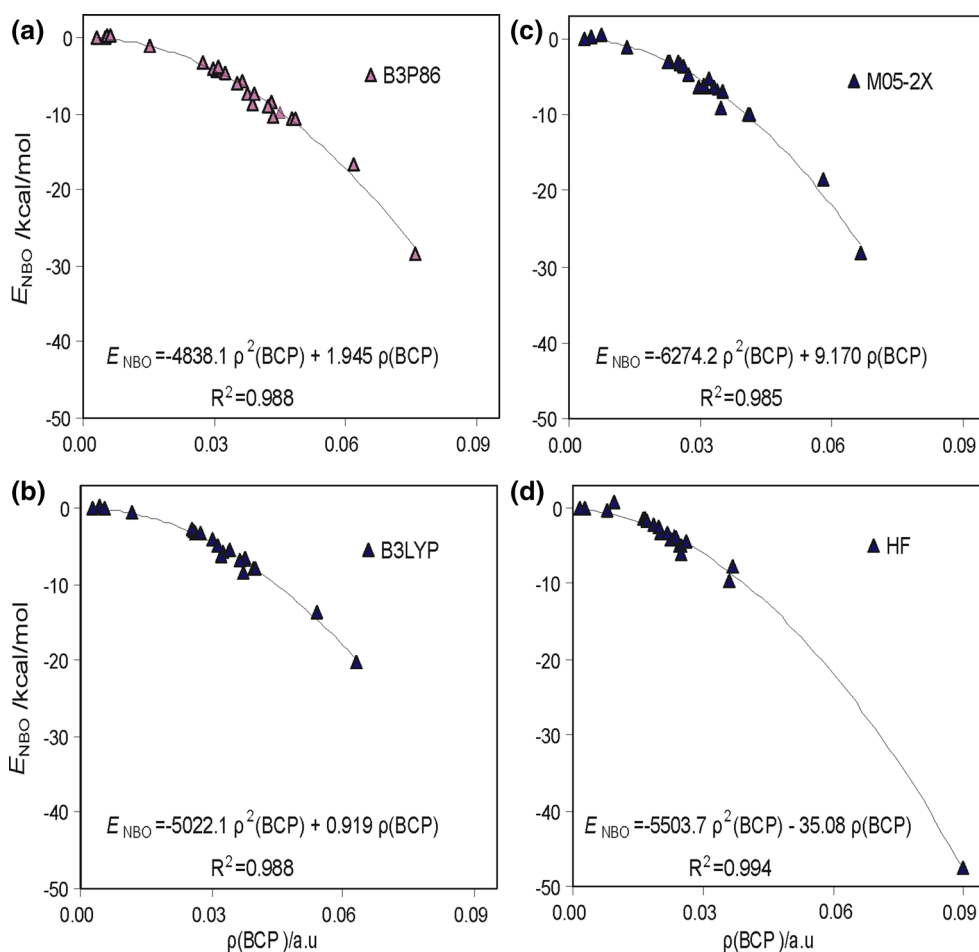
$$E_{NBO} = -4838.1\, \rho^2(BCP) + 1.945\, \rho(BCP)$$
$$R^2 = 0.988$$

$$E_{NBO} = -6274.2\, \rho^2(BCP) + 9.170\, \rho(BCP)$$
$$R^2 = 0.985$$

$$E_{NBO} = -5022.1\, \rho^2(BCP) + 0.919\, \rho(BCP)$$
$$R^2 = 0.988$$

$$E_{NBO} = -5503.7\, \rho^2(BCP) - 35.08\, \rho(BCP)$$
$$R^2 = 0.994$$
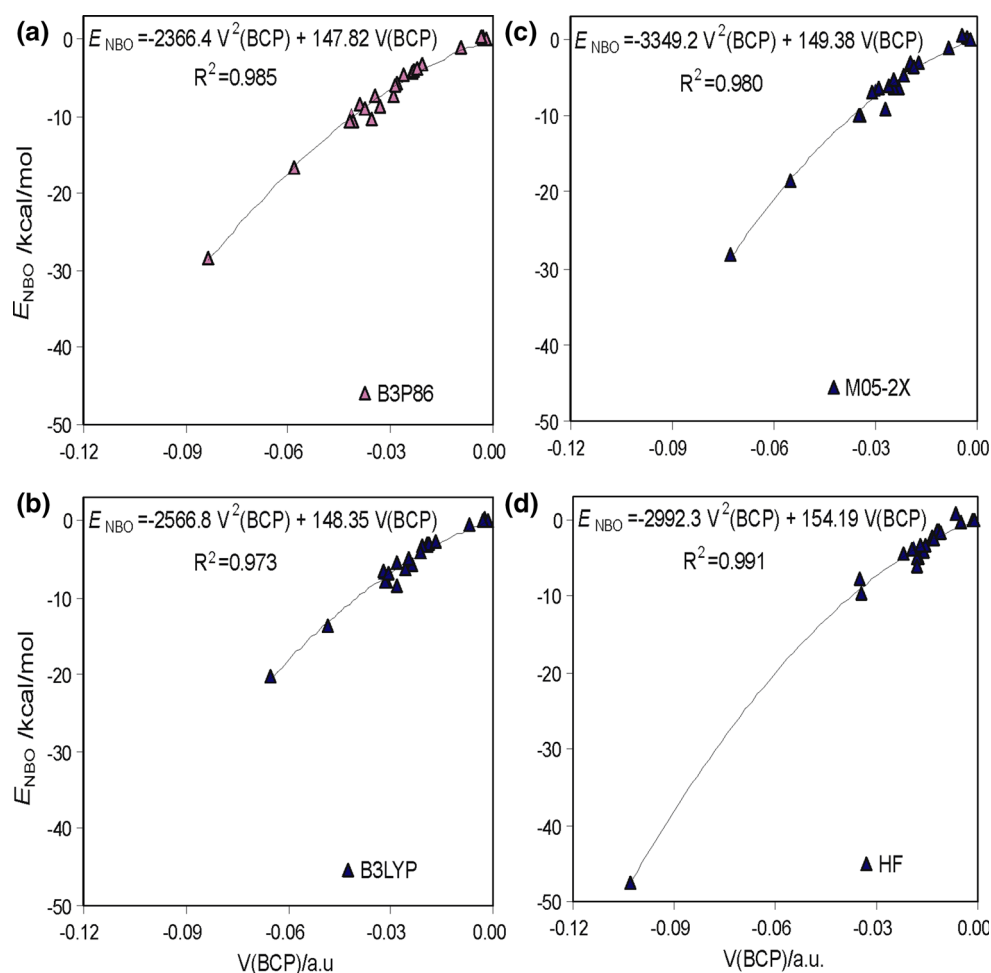
between both units due to the reorganization of electron
density upon the complex formation. It has been qualita-
tively or semi-quantitatively evaluated in a number of
publications [11–13, 23–32] and was correlated with the
binding energy. However, it appeared that the total charge
transfer was only one of a few physical terms bringing
about stabilization energy of the complexes [33–40].

The H-bonded complexes were also characterized with
the aim of the quantum theory of atoms in molecules
(QTAIM) [41] that serves as a tool for the topological
analysis of electron densities and has been also used to
study HBs in various canonical and noncanonical DNA
base pairs (27 dimers) [42]. Correlations of electron density
properties at the bond critical point (BCP) of HB with its
energy have been mainly applied to complexes of mole-
cules bound by a single hydrogen bond. In cases where the
complexes can be classified in families according to the
various proton acceptors (Y in H···Y), the correlations
between the different parameters (derived from the
QTAIM theory) on one hand, and energetic properties on
the other hand, have been particularly found for homoge-
neous samples [5, 11, 23, 28, 31, 43–48].

Summarizing, there have been many attempts to correlate
the HB strength with its structural (geometrical) or electronic
parameters. The obtained relations well describe discussed
characteristics for homogeneous types of interactions [49].
For this purpose the NBO analysis in combination with the
QTAIM method have also been applied [50]. However,
energy of particular HB was characterized only by one—the
attractive component ($E^{(2)}$ or $E_{n-\sigma*}$ in the present notation) of
intermolecular interaction. The good correlations between
$E^{(2)}$ and the electron density at the H-bond critical point,
$\rho(BCP)$, were obtained separately for the NH···O and NH···N
data. The H-bond energy evaluated according to the NBO
methodology, E_{NBO}, renders interactions between orbitals
directly engaged in a HB (for X–H···Y interaction: n_Y, $\sigma*_{XH}$
and σ_{XH}). It is named here as energy of an individual or
single HB energy. Its attractive contribution, $E_{n-\sigma*}$, is due to
the partial charge transfer between the n_Y and $\sigma*_{XH}$ orbitals
and is accompanied by the repulsive contribution, $E_{\sigma-n}$,
between the filled n_Y and σ_{XH} orbitals interaction.

The aim of the present paper was to find correlations
between simply available parameters based on the QTAIM
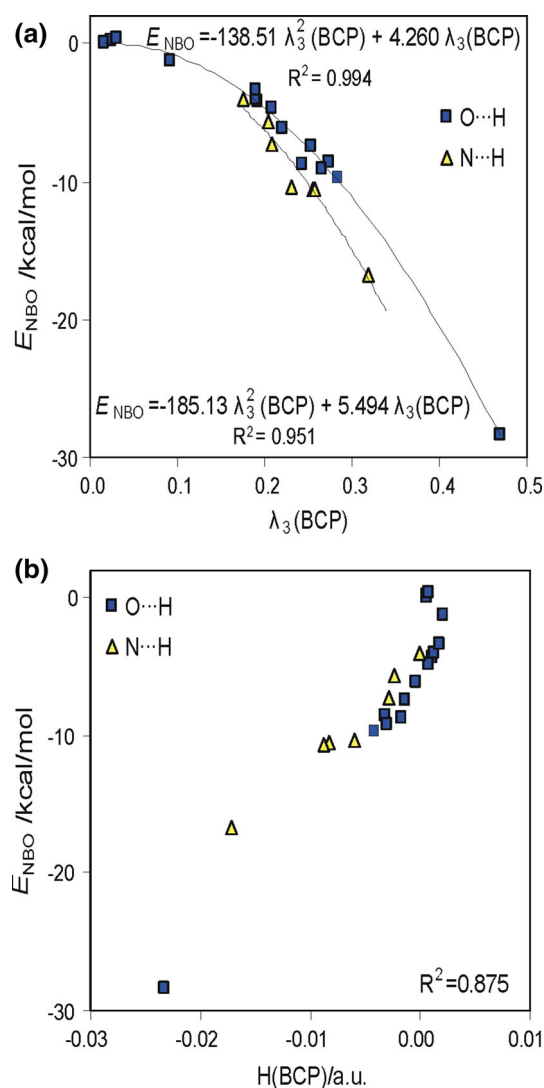and NBO methodologies, for characterizing contribution of

Fig. 3 Relationship between the energy of a single H-bond, E_{NBO}, and **a** curvature of the electron density λ_3 at BCP, $\lambda_3(BCP)$, **b** the total electron energy density at BCP, H(BCP), for G–C, A–T, G–U, A–U and substituted derivatives R1G-CR2 and R1A-TR2 pairs; B3P86/6-311++G(d,p) results. *Squares* indicate N–H···O and C–H···O interactions, whereas *triangles* signify N–H···N H-bonds

the H-bonds to the intermolecular interactions which appear in DNA and RNA base pairs: N–H···O, O–H···O, and C–H···O. We hoped to find good correlations for a single data set concerning bonds of all three types (the so called heterogeneous data set). To this end, the NBO energies of the individual H-bonds were correlated with some QTAIM parameters.

Methodology

The geometry of the nucleic acid base pairs was minimized at the theoretical levels HF and DFT [51]. In the case of the DFT method, the hybrid functional of Becke [52] with Lee,

Yang, and Parr gradient correction [53], B3LYP, and with the gradient correction of Perdew [54], B3P86, as well as the recently designed M05-2X functional [55] were applied. The latter provided a very good performance for the closed-shell organic systems [56] and the noncovalent interactions [57]. The B3P86/6-311++G(d,p) level was recently used to investigate the geometric, electronic, and energetic properties of 31 canonical and wobble base pairs [58], and this level of theory has also been used for substituted G–C and A–T derivatives. Moreover, it has been found that this functional is one among five functionals (out of the 44 investigated) that provides the best performance for H-bonding [59].

For the geometry optimization, NBO analysis, and generation of the wave function for the QTAIM analysis [60] the triple-ζ split-valence basis set, denoted as 6-311++G(d,p) according to the Pople's nomenclature [61] was applied. Subsequently, the NBO method with the NBO-5.G program [62] was applied to study the electron distribution among the individual "natural" orbitals in a system and to estimate the individual H-bond strengths [14]. The calculations were performed using the Gaussian 03 and 09 suite of programs [63, 64]. The QTAIM analysis was performed to calculate the electron density (ρ), the potential electron energy density V(BCP), the total electron energy density H(BCP) and curvature of the electron density $\lambda_3(BCP)$ at BCPs. The QTAIM analysis was carried out using the AIMPAC package [65].

According to the NBO analysis, X–H···Y H-bonding corresponds to an intermolecular donor–acceptor interaction between a lone pair (n) of the Lewis base (the H-bond acceptor, Y; in our case, an oxygen or nitrogen atom) and the proximate antibonding orbital (σ^*) of the Lewis acid (the H-bond donor, X–H; in our case, N–H or C–H). The strength of this single interaction, E_{NBO}, can be estimated as

$$E_{NBO} = E^{(2)} + E_{\sigma-n} \qquad (1)$$

where $E^{(2)} = E_{n-\sigma^*}$ means the second-order stabilization energy of the partial CT $n_Y \rightarrow \sigma_{X-H^*}$ interaction, and $E_{\sigma-n}$ denotes the steric repulsion energy of σ_{X-H} and n_Y orbitals.

To challenge the method, we included to the investigated set of complexes two pairs (G–C and A–T) substituted by NH_3^+ or OH_2^+, for which stronger perturbations of atomic structure were expected.

Results and discussion

Nucleic acid base pairs, the most important systems with multiple HBs, were chosen to find an interdependence between parameters characterizing intermolecular interactions that allows to estimate the strength of particular HBs.

Table 1 Values of the electron density ρ(BCP), the potential energy density V(BCP) and energy of a single H-bond, E_{NBO}, calculated at the HF/6-311++G(d,p) level

HF	H-bond	ρ(BCP)/a.u.		V(BCP)/a.u.		E_{NBO}/kcal/mol	
G–C	N–H···O	0.02332	*a > b > c*	−0.01881	*a > b > c*	−3.57	b > a > c
	N–H···N	0.02262		−0.01576		−4.26	
	N–H···O	0.01852		−0.01370		−2.11	
A–T	N–H···O	0.01605	b > a > c	−0.01144	b > a > c	−1.35	b > a > c
	N–H···N	0.02470		−0.01775		−4.95	
	C–H···O	0.00275		−0.00170		0.02	
NH$_3^+$–GC	N–H···O	0.01681	*c > b > a*	−0.01221	*c > b > a*	−1.53	b > c > a
	N–H···N	0.02495		−0.01797		−6.00	
	N–H···O	0.02599		−0.02181		−4.39	
GC–OH$_2^+$	N–H···O	0.03604	a > b > c	−0.03462	a > b > c	−9.56	a > b > c
	N–H···N	0.01718		−0.01095		−1.66	
	N–H···O	0.00810		−0.00503		−0.38	
NH$_3^+$–AT	N–H···O	0.02177	a > b > c	−0.01710	a > b > c	−3.29	a > b > c
	N–H···N	0.01979		−0.01318		−2.44	
	C–H···O	0.00169		−0.00097		0.01	
AT–OH$_2^+$	N–H···O	0.03678	b > a > c	−0.03483	b > a > c	−7.65	b > a > c
	N–H···N	0.08990		−0.10286		−47.53	
	C–H···O	0.00967		−0.00627		0.78	
A–U	N–H···O	0.01613	b > a> c	−0.01151	b > a> c	−1.47	b > a> c
	N–H···N	0.02488		−0.01792		−5.03	
	C–H···O	0.00272		−0.00168		0.02	
G–U	N–H···O	0.02002	b > a	−0.01530	b > a	−3.19	b > a
	N–H···O	0.02379		−0.01949		−3.78	

In columns 4, 6 and 8, the ordering of ρ(BCP), V(BCP) and E_{NBO} for individual bonds is indicated. Italic letters in columns 4 and 6 denotes discrepancy with NBO results

For this purpose following systems were taken into account: two Watson–Crick base pairs, guanine–cytosine (G–C) and adenine–thymine (A–T); these pairs substituted by one of two substituents, NH$_3^+$ or OH$_2^+$; adenine–uracil (A–U) occurring in RNA and a wobble pair guanine–uracil (G–U). The respective hydrogen bonds are marked as **a**, **b**, **c**, in Schemes 1 and 2. Obtained characteristics of individual HBs are presented in Figs. 1, 2 and 3, whereas values of calculated parameters are gathered in Tables 1, 2, 3 and 4 and S1–S2, the latter in Supplementary Information.

Plots of E_{NBO} versus ρ(BCP) for 23 HBs occurring in the base pairs presented in Schemes 1 and 2, are shown in Fig. 1. The Figure shows that the energy increment due to the transfer of charge within a confined space of the X–H···Y bond is monotonically dependent on the electron density at the critical point of the bond. Moreover, we observe that the points representing bonds with different X and Y, e.g. N–H···O, N–H···N, and C–H···O lie on the same line. Therefore, the interdependence of the parameters E_{NBO} and ρ(BCP), belonging to quite different descriptions of the H-bonds, is a universal one, at least within a set of the bonds found in the DNA base pairing. This finding

points at the essential relevancy of the two approaches to the interpretation of the H-bonding phenomenon. A comparison of relationships presented in Fig. 1 shows that the four plots are similar and characterized by approximate correlation coefficients despite that one approach detects only electron densities on the appropriate orbitals of the donor and acceptor and their interaction, and the second approach detects the electron density at a point of its zero gradient, lying along the H···Y line. A conclusion can be made that both determinants of an individual H-bond strength evaluate quantitatively the bonds in a congruent manner and that the accuracy of results is not very dependent on the calculation level.

It appeared that similar relationships were also observed for E_{NBO} and another QTAIM parameter, the potential energy density at BCP of hydrogen bond, V(BCP). Plots of E_{NBO} and V(BCP) are shown in Fig. 2. Analysis of the plots demonstrates that the conclusion arrived at the last sentence of preceding paragraph can also be held in the case when V(BCP) is compared with the E_{NBO}.

As there were other parameters proposed as descriptors of the total binding energy of the HB complexes, namely the total electron energy density H(BCP) [40, 42] and

Table 2 Values of the electron density ρ(BCP), the potential energy density V(BCP) and energy of a single H-bond, E_{NBO}, calculated at the B3P86/6-311++G(d,p) level

B3P86	H-bond	ρ(BCP)/a.u.		V(BCP)/a.u.		E_{NBO}/kcal/mol	
G–C	N–H···O	0.04480	a > b > c	−0.04127	a > b > c	−9.74	a > b > c
	N–H···N	0.03769		−0.02928		−7.32	
	N–H···O	0.03032		−0.02383		−4.28	
A–T	N–H···O	0.02989	b > a > c	−0.02345	b > a > c	−4.02	b > a > c
	N–H···N	0.04778		−0.04079		−10.53	
	C–H···O	0.00500		−0.00289		0.13	
NH_3^+–GC	N–H···O	0.03240	b > c > a	−0.02641	c > b > a	−4.77	b > c > a
	N–H···N	0.04341		−0.03534		−10.41	
	N–H···O	0.04283		−0.03894		−8.56	
GC–OH_2^+	N–H···O	0.07590	a > b > c	−0.08327	a > b > c	−28.39	a > b > c
	N–H···N	0.03079		−0.02226		−3.96	
	N–H···O	0.01533		−0.00954		−1.21	
NH_3^+–AT	N–H···O	0.04214	a > b > c	−0.03770	a > b > c	−9.13	a > b > c
	N–H···N	0.03653		−0.02829		−5.63	
	C–H···O	0.00321		−0.00178		0.02	
AT–OH_2^+	N–H···O	0.03510	b > a > c	−0.02885	b > a > c	−6.14	b > a > c
	N–H···N	0.06172		−0.05818		−16.73	
	C–H···O	0.00614		−0.00353		0.34	
A–U	N–H···O	0.02723	b > a > c	−0.02066	b > a > c	−4.26	b > a > c
	N–H···N	0.04856		−0.04178		−10.79	
	C–H···O	0.00550		−0.00315		0.14	
G–U	N–H···O	0.03856	*b > a*	−0.03323	*b > a*	−8.73	a > b
	N–H···O	0.03926		−0.03470		−7.44	

In columns 4, 6 and 8, the ordering of ρ(BCP), V(BCP) and E_{NBO} for individual bonds is indicated. Italic letters in columns 4 and 6 denotes discrepancy with NBO results

positive curvature of electron density, λ_3(BCP) [37], it was interesting to check correlations of these parameters with the energy of individual HB, i.e. the energy of orbital interactions provided by the NBO analysis. Therefore, we plotted H(BCP) and λ_3(BCP) versus E_{NBO} for our set of the N–H···O, N–H···N, and C–H···O bonds (calculations at the B3P86/6-311++G(d,p) level). Indeed, as shown in Fig. 3, the HB energy was correlated with the two descriptors to some degree, yet the correlation coefficients were poorer than these shown in Figs. 1 and 2. Moreover, data belonging to the H···N and H···O bonds were rather separated, so none of the two descriptors could be selected for the comparison of the hydrogen bonds of different types in the investigated DNA base pairs. Of the two plots given in Fig. 3, the first is characterized by higher correlation coefficient. The calculations were repeated at the M05-2X/6-311++G(d,p) level and the results were virtually the same.

Taking into consideration that augmentation of ρ(BCP) and V(BCP) goes hand in hand with the increase of the single HB energy (Figs. 1, 2), we compared the ordering of the latter predicted by the two methods used, within the individual base pairs, shown in Schemes 1 and 2.

The values of the electron density ρ(BCP), of the potential electron energy density V(BCP) and of E_{NBO} according to Eq. (1) are displayed in Tables 1, 2, 3 and 4, for different calculation levels applied. The values show that the energy sequence of two of the three bonds may differ, as presented in columns 4, 6 and 8. This is so for two pairs at the HF level: G–C and NH_3^+-G–C (Table 1), for two pairs at the B3LYP level: NH_3^+-G–C and G–U (Table 3), for three pairs at the M05-2X level: NH_3^+-G–C, NH_3^+-A–T, G–U (Table 4) and for only one pair, G–U, at the B3P86 level (Table 2). A comparison of the plots of E_{NBO} versus V(BCP) points to the same results at the HF, B3P86 and B3LYP levels; at M05-2X there is one pair less for which the V(BCP) and E_{NBO} orderings are inconsistent.

It is evident that the single HB energy forecast based on the ρ(BCP) value is generally accurate except of the cases when two bonds are characterized by a very similar values of ρ(BCP), for example 0.0373 and 0.0375 calculated at B3LYP for two HBs in NH_3^+-G–C. The best functional for our purpose was found B3P86, with which the disagreement is found for only one pair for both QTAIM parameters. When such a comparison was made based on λ_3 as an QTAIM parameter the inversion of the bond sequence

Table 3 Values of the electron density ρ(BCP), the potential energy density V(BCP) and energy of a single H-bond, E_{NBO}, calculated at the B3LYP/6-311++G(d,p) level

B3LYP	H-bond	ρ(BCP)/a.u.		V(BCP)/a.u.		E_{NBO}/kcal/mol	
G–C	N–H···O	0.03755	a > b > c	−0.03215	a > b > c	−6.84	a > b > c
	N–H···N	0.03252		−0.02348		−5.86	
	N–H···O	0.02621		−0.01936		−3.22	
A–T	N–H···O	0.02586	b > a > c	−0.01914	b > a > c	−2.93	b > a > c
	N–H···N	0.03954		−0.03091		−7.89	
	C–H···O	0.00416		−0.00235		0.19	
NH_3^+–GC	N–H···O	0.02720	c > b > a	−0.02062	c > b > a	−3.30	b > c > a
	N–H···N	0.03733		−0.02826		−8.35	
	N–H···O	0.03747		−0.03218		−6.66	
GC–OH_2^+	N–H···O	0.06299	a > b > c	−0.06528	a > b > c	−20.2	a > b > c
	N–H···N	0.02551		−0.01682		−2.84	
	N–H···O	0.01183		−0.00689		−0.66	
NH_3^+–AT	N–H···O	0.03632	a > b > c	−0.03060	a > b > c	−6.81	a > b > c
	N–H···N	0.03011		−0.02119		−4.13	
	C–H···O	0.00258		−0.00136		0.06	
AT–OH_2^+	N–H···O	0.03146	b > a > c	−0.02465	b > a > c	−5.03	b > a > c
	N–H···N	0.05409		−0.04838		−13.62	
	C–H···O	0.00544		−0.00307		0.06	
A–U	N–H···O	0.02572	b > a > c	−0.01899	b > a	−3.08	b > a > c
	N–H···N	0.04001		−0.03142		−8.04	
	C–H···O	0.00416		−0.00236		0.11	
G–U	N–H···O	0.03204	*b > a*	−0.02558	*b > a*	−6.16	a > b
	N–H···O	0.03394		−0.02824		−5.57	

In columns 4, 6 and 8, the ordering of ρ(BCP), V(BCP) and E_{NBO} for individual bonds is indicated. Italic letters in columns 4 and 6 denotes discrepancy with NBO results

Table 4 Values of the electron density ρ(BCP), the potential energy density V(BCP) and energy of a single H-bond, E_{NBO}, calculated at the M05-2X/6-311++G(d,p) level

M05-2X	H-bond	ρ(BCP)/a.u.		V(BCP)/a.u.		E_{NBO}/kcal/mol	
G–C	N–H···O	0.03400	a > b > c	−0.029905	a > b > c	−6.79	a > b > c
	N–H···N	0.03059		−0.022872		−6.41	
	N–H···O	0.02515		−0.019643		−3.44	
A–T	N–H···O	0.02279	b > a > c	−0.017105	b > a > c	−2.74	b > a > c
	N–H···N	0.04079		−0.034223		−9.89	
	C–H···O	0.00501		−0.002973		0.16	
NH_3^+–GC	N–H···O	0.02482	c > b > a	−0.019477	c > b > a	−3.19	b > c > a
	N–H···N	0.03470		−0.027000		−9.08	
	N–H···O	0.03493		−0.031189		−6.82	
GC–OH_2^+	N–H···O	0.06642	a > b > c	−0.072749	a > b > c	−28.29	a > b > c
	N–H···N	0.02628		−0.018804		−3.55	
	N–H···O	0.01318		−0.008294		−1.08	
NH_3^+–AT	N–H···O	0.03091	*b > a > c*	−0.025908	a > b > c	−6.17	a > b > c
	N–H···N	0.03180		−0.024562		−5.17	
	C–H···O	0.00339		−0.001944		0.05	
AT–OH_2^+	N–H···O	0.02724	b > a > c	−0.021417	b > a > c	−4.69	b > a > c
	N–H···N	0.05801		−0.055231		−18.52	
	C–H···O	0.00721		−0.004293		0.39	
A–U	N–H···O	0.02277	b > a > c	−0.017090	b > a> c	−2.94	b > a > c
	N–H···N	0.04121		−0.034687		−10.1	
	C–H···O	0.00506		−0.003009		0.17	
G–U	N–H···O	0.02962	*b > a*	−0.024436	*b > a*	−6.42	a > b
	N–H···O	0.03314		−0.029085		−6.38	

In columns 4, 6 and 8, the ordering of ρ(BCP), V(BCP) and E_{NBO} for individual bonds is indicated. Italic letters in columns 4 and 6 denotes discrepancy with NBO results

was found in two cases (calculations at the B3P86/6-311++G(d,p) and M05-2XD/6-311++G(d,p) levels). However, the agreement of ordering of the single HB energies based on the H and E_{NBO} values, calculated at the M05-2X level, was much poorer. The corresponding Tables (S1 and S2) are given in the Supplementary Information.

Conclusions

This study was dedicated to correlations of energies of the individual hydrogen bonds, E_{NBO} (especially in complexes possessing multiple bonds), with the QTAIM characteristics of electron density at the H-bond critical point. Special attention has been paid to differentiate the NBO energies of individual H-bonds from the total stabilization energy of the complexes. Three types of intermolecular interactions, NH···O, NH···N, and CH···O, which are present in DNA/RNA base pairs, were analyzed.

(1) The best correlations were found with the electron density ρ and energy density V at the hydrogen bond critical point (BCP), provided by the QTAIM methodology.

(2) Among other characteristics at the BCP offered by QTAIM, the positive curvature of the electron density λ_3 and the total electron energy density H were also correlated with E_{NBO}, but the correlations were poorer than those of ρ or V with E_{NBO}.

(3) The ordering of energies of individual H-bonds determined by NBO approach generally coincides with the sequence offered by the (ρ, V, λ_3) QTAIM parameters, however, the sequence can be inverted when two bonds are characterized by a very similar QTAIM parameters or E_{NBO} values.

(4) The best agreement of the two gauges of the single HB energies was attained when electron density or potential energy density at the BCP was selected and the values to be compared were calculated with the B3P86 functional.

The presented procedure is not limited only to DNA or RNA nucleic acids. It could also be applied to various cases where the intermolecular hydrogen bonds occur, especially if several HBs are present in the same molecule. It allows for the joint comparison of the H-bonds of different types, within the so-called heterogeneous samples. The method could also be useful in the cases characterized by a crucial role of environmental effects which cannot be omitted from consideration.

Summarizing, the proposed procedure can be applied to estimate the part of intermolecular interactions energy attributed to individual hydrogen bonds.

References

1. Swart M, Fonseca Guerra C, Bickelhaupt FM (2004) J Am Chem Soc 126:16718–16719
2. Asensio A, Kobko N, Dannenberg JJ (2003) J Phys Chem A 107:6441–6443
3. Grunenberg J (2004) J Am Chem Soc 126:16310–16311
4. Dong H, Hua W, Li S (2007) J Phys Chem A 111:2941–2945
5. Espinosa E, Molins E, Lecomte C (1998) Chem Phys Lett 285:170–173
6. Matta CF, Castillo N, Boyd RJ (2006) J Phys Chem B 110:563–578
7. Ebrahimi A, Habibi Khorassani SM, Delarami H (2009) Chem Phys 365:18–23
8. Ebrahimi A, Habibi Khorassani SM, Delarami H, Esmaeel H (2010) J Comput Aided Mol Des 24:409–416
9. Szatylowicz H, Sadlej-Sosnowska N (2010) J Chem Inf Model 50:2151–2161
10. Fliegl H, Lehtonen O, Sundholm D, Kaila VRI (2011) Phys Chem Chem Phys 13:434–437
11. Nikolaienko TY, Bulavina LA, Hovorun DM (2012) Phys Chem Chem Phys 14:7441–7447
12. Brovarets OO, Hovorun DM (2014) J Biomol Struct Dyn 32:127–154
13. Brovarets OO, Hovorun DM (2014) J Biomol Struct Dyn 32:1474–1499
14. Weinhold F, Landis CR (2005) Valency and bonding. A natural bond orbital donor-acceptor perspective. Cambridge University Press, Cambridge
15. Badenhoop JK, Weinhold F (1997) J Chem Phys 107:5406–5421
16. Badenhoop JK, Weinhold F (1997) J Chem Phys 107:5422–5432
17. Badenhoop JK, Weinhold F (1999) Int J Quantum Chem 72:269–280
18. Weinhold F, Klein RA (2012) Mol Phys 110:565–579
19. Piela L (2013) Ideas of quantum chemistry, 2nd edn. Elsevier, Philadelphia, pp 802–805
20. Scheiner S (1997) Hydrogen bonding, a theoretical perspective. Oxford University Press, New York
21. Scheiner S, Kar T (2002) J Phys Chem A 106:1784–1789
22. Carroll MT, Bader RWF (1988) Mol Phys 65:695–722
23. Grabowski SJ (2002) J Mol Struct 615:239–245
24. Parthasarathi R, Subramanian V (2006) Characterization of hydrogen bonding: from van der Waals interactions to covalency: unified picture of hydrogen bonding based on electron density topography analysis. In: Grabowski SJ (ed) Hydrogen bonding: new insights. Springer, New York, pp 1–50
25. Grabowski SJ, Sokalski WA, Dyguda E, Leszczyński J (2006) J Phys Chem B 110:6444–6446

26. Oliveira BG, Pereira FS, de Araújo RCMU, Ramos MN (2006) Chem Phys Lett 427:181–184
27. Poater J, Fradera X, Solà M (2003) Chem Phys Lett 369:248–255
28. Mohajeri A, Nobandegani FF (2008) J Phys Chem A 112:281–295
29. Grabowski SJ (2011) Chem Rev 111:2597–2625
30. Fuster F, Grabowski SJ (2011) J Phys Chem A 115:10078–10086
31. Mata I, Alkorta I, Espinosa E, Molins E (2011) Chem Phys Lett 507:185–189
32. Li X, Wang Y, Zheng S, Meng L (2012) Struct Chem 23:1233–1240
33. Mo Y, Gao J (2001) J Phys Chem A 105:6530–6536
34. Mo Y (2006) J Mol Model 12:665–672
35. Fonseca Guerra C, Bickelhaupt FM, Snijders JG, Baerends EJ (1999) Chem Eur J 5:3581–3594
36. Fonseca Guerra C, Bickelhaupt FM (1999) Angew Chem Int Ed 38:2942–2945
37. Fonseca Guerra C, van der Wijst T, Bickelhaupt FM (2006) Chem Phys Chem 7:1971–1979
38. Ran J, Hobza P (2009) J Phys Chem B 113:2933–2936
39. Fonseca Guerra C, Bickelhaupt FM (2002) Angew Chem Int Ed 41:2092–2095
40. Fonseca Guerra C, Bickelhbaupt FM, Baerends EJ (2002) Cryst Growth Des 2:239–245
41. Bader RWF (1990) Atoms in molecules: a quantum theory. Clarendon Press, Oxford
42. Parthasarathi R, Amutha R, Subramanian V, Nair BU, Ramasami T (2004) J Phys Chem A 108:3817–3828
43. Gálvez O, Gómez PC, Pacios LF (2001) J Chem Phys 115:11166–11184
44. Espinosa E, Souhassou M, Lachekar H, Lecomte C (1999) Acta Cryst B55:563–572
45. Grabowski SJ (2001) J Phys Chem A 105:10739–10746
46. Grabowski SJ (2001) J Mol Struct 562:137–143
47. Espinosa ED, Alkorta I, Elguero J, Molins E (2002) J Chem Phys 117:5529–5542
48. Hugas D, Simon S, Duran M (2007) J Phys Chem A 111:4506–4512
49. Rozas I (2007) Phys Chem Chem Phys 9:2782–2790
50. Rozas I, Alkorta I, Elguero J (2004) J Phys Chem B 108:3335–3341
51. Cramer CJ (2003) Essentials of computational chemistry. Wiley, London
52. Becke AD (1988) Phys Rev A: At Mol Opt Phys 38:3098–3100
53. Lee C, Yang W, Parr RG (1988) Phys Rev B: Condens Matter Mater Phys 37:785–789
54. Perdew JP (1986) Phys Rev B: Condens Matter Mater Phys 33:8822–8824
55. Zhao Y, Schultz NE, Truhlar DG (2006) J Chem Theory Comput 2:364–382
56. Zhao Y, Truhlar DG (2006) J Phys Chem A 110:10478–10486
57. Zhao Y, Truhlar DG (2008) Acc Chem Res 41:157–167
58. Sadlej-Sosnowska N (2009) J Mol Struct: THEOCHEM 913:270–276
59. Zhao Y, Truhlar DG (2005) J Chem Theory Comput 1:415–432
60. Biegler König J, Schönbohm F (2000) AIM 2000 version 2.0. http://www.aim2000.de
61. Krishnan R, Binkley JS, Seeger R, Pople J (1980) J Chem Phys 772:650–654
62. Glendening ED, Badenhoop JK, Reed AE, Carpenter JE, Bohmann JA, Morales CM, Weinhold F (2004) NBO 5.0G. Theoretical Chemistry Institute, University of Wisconsin, Madison http://www.chem.wisc.edu/~nbo5
63. Frisch MJ, Trucks GW, Schlegel HB, Scuseria GE, Robb MA, Cheeseman JR, Jr. Montgomery JA, Vreven T, Kudin KN, Burant JC, Millam JM, Iyengar SS, Tomasi J, Barone V, Mennucci B, Cossi M, Scalmani G, Rega N, Petersson GA, Nakatsuji H, Hada M, Ehara M, Toyota K, Fukuda R, Hasegawa J, Ishida M, Nakajima T, Honda Y, Kitao O, Nakai H, Klene M, Li X, Knox JE, Hratchian HP, Cross JB, Adamo C, Jaramillo J, Gomperts R, Stratmann RE, Yazyev O, Austin AJ, Cammi R, Pomelli C, Ochterski JW, Ayala PY, Morokuma K, Voth GA, Salvador P, Dannenberg JJ, Zakrzewski VG, Dapprich S, Daniels AD, Strain MC, Farkas O, Malick DK, Rabuck AD, Raghavachari K, Foresman JB, Ortiz JV, Cui Q, Baboul AG, Clifford S, Cioslowski J, Stefanov BB, Liu G, Liashenko A, Piskorz P, Komaromi I, Martin RL, Fox DJ, Keith T, Al-Laham MA, Peng CY, Nanayakkara A, Challacombe M, Gill PMW, Johnson B, Chen W, Wong MW, Gonzalez C, Pople JA (2004) Gaussian 03, Revision C.02; Gaussian, Inc.: Wallingford, CT
64. Frisch MJ, Trucks GW, Schlegel HB, Scuseria GE, Robb MA, Cheeseman JR, Scalmani G, Barone V, Mennucci B, Petersson GA, Nakatsuji H, Caricato M, Li X, Hratchian HP, Izmaylov AF, Bloino J, Zheng G, Sonnenberg JL, Hada M, Ehara M, Toyota K, Fukuda R, Hasegawa J, Ishida M, Nakajima T, Honda Y, Kitao O, Nakai H, Vreven T, Montgomery Jr JA, Peralta JE, Ogliaro F, Bearpark M, Heyd JJ, Brothers E, Kudin KN, Staroverov VN, Kobayashi R, Normand J, Raghavachari K, Rendell A, Burant JC, Iyengar SS, Tomasi J, Cossi M, Rega N, Millam MJ, Klene M, Knox JE, Cross JB, Bakken V, Adamo C, Jaramillo J, Gomperts R, Stratmann RE, Yazyev O, Austin AJ, Cammi R, Pomelli C, Ochterski JW, Martin RL, Morokuma K, Zakrzewski VG, Voth GA, Salvador P, Dannenberg JJ, Dapprich S, Daniels AD, Farkas Ö, Foresman JB, Ortiz JV, Cioslowski J, Fox DJ (2009) GAUSSIAN 09 (Revision B.01) Gaussian Inc, Wallingford CT
65. Bader RWF (1991) AIMPAC, suite of programs for the theory of atoms in molecules. McMaster University, Hamilton